Endocrine, *vol. 18, no. 1, 1–12, June 2002* 0969–711X/02/18:1–12/$13.00

Regulation of IRS-1/SHP2 Interaction and AKT Phosphorylation in Animal Models of Insulin Resistance

Maria Helena M. Lima,[1] Mirian Ueno,[1] Ana Cláudia P. Thirone,[1] Eduardo M. Rocha,[1] Carla Roberta O. Carvalho,[2] and Mário J.A.Saad[1]

[1]Department of Internal Medicine, State University of Campinas (UNICAMP), Campinas, Brazil; and [2]Department of Physiology and Biophysics (USP), São Paulo, Brazil

Insulin stimulates tyrosine kinase activity of its receptor, resulting in phosphorylation of its cytosolic substrate, insulin receptor substrate-1, which, in turn, associates with proteins containing SH2 domains, including phosphatidylinositol 3-kinase (PI 3-kinase) and the phosphotyrosine phosphatase SHP2. The regulation of these associations in situations of altered insulin receptor substrate-1 (IRS-1) phosphorylation was not yet investigated. In the present study, we investigated insulin-induced IRS-1/SHP2 and IRS-1/PI 3-kinase associations and the regulation of a downstream serine–kinase AKT/PKB in liver and muscle of three animal models of insulin resistance: STZ diabetes, epinephrine-treated rats, and aging, which have alterations in IRS-1 tyrosine phosphorylation in common. The results demonstrated that insulin-induced IRS-1/PI 3-kinase association has a close correlation with IRS-1 tyrosine phosphorylation levels, but insulin-induced IRS-1/SHP2 association showed a modulation that did not parallel IRS-1 phosphorylation, with a tissue-specific regulation in aging. The integration of the behavior of IRS-1/PI 3-kinase and with IRS-1/SHP2 associations may be important for insulin signaling downstream as AKT phosphorylation. In conclusion, the results of the present study demonstrated that insulin-induced IRS-1/SHP2 association can be regulated in insulin-sensitive tissues of animal models of insulin resistance and may have a role in the control of AKT phosphorylation, which may be implicated in the control of glucose metabolism.

Key Words: Insulin receptor substrate-1; phosphotyrosine phosphatase; signal transduction; insulin resistance; SHP2.

Introduction

Insulin resistance is defined as a subnormal biologic response to a given concentration of insulin and is characteristic of many disease states, including type 2 diabetes, uncontrolled type 1 diabetes, aging, and excess of epinephrine. Although various defects in insulin action have been reported in these conditions, the exact molecular mechanisms involved in the insulin resistance have not been adequately elucidated.

The insulin receptor is the principal mediator of insulin action on cellular mitogenic and metabolic processes. The insulin receptor β-subunit, which contains an intrinsic tyrosine kinase, undergoes tyrosyl autophosphorylation and is activated in response to insulin binding to the extracellular α-subunit *(1)*. This interaction further enhances the tyrosine kinase activity of the receptor toward other intermediate molecules, including insulin receptor substrate-1 (IRS-1) *(2, 3)*. After insulin stimulation, IRS-1 associates with several proteins, including phosphatidylinositol (PI) 3-kinase, phosphotyrosine phosphatase SHP2, and adapter molecules like Nck, Grb2, and Fyn *(4–6)*. The enzyme PI 3-kinase has been shown to play a critical role in many of the metabolic effects of the insulin, including stimulation of glucose transport, activation of glycogen synthase, and inhibition of phosphoenolpyruvate carboxykinase (PEPCK), the key enzyme of gluconeogenesis *(7)*. Different approaches have demonstrated that AKT/PKB, a serine–threonine kinase with a pleckstrin homology domain, is functionally located downstream of PI 3-kinase *(8–12)*.

SHP2 is an SH2 domain-containing tyrosine phosphatase that associates with the COOH-terminal tyrosine phosphorylation sites of IRS-1 in cultured cells, and this association increases the phosphatase activity of SHP2 in vitro *(13)*. We have recently demonstrated that insulin induces IRS-1/SHP2 association in vivo in rat tissues, suggesting that this pathway is physiologically relevant *(14)*. However, the regulation of this association in situations of altered IRS-1 phosphorylation was not investigated. In the present study, we investigated insulin-induced IRS-1/SHP2 association and AKT/PKB phosphorylation in liver and muscle of three animal models of insulin resistance: streptozotocin (STZ) diabetes, epinephrine-treated rats, and aging, which have in common alteration in IRS-1 tyrosine phosphorylation *(15–17)*.

Received September 18, 2001; Revised December 12, 2001; Accepted February 15, 2002.

Author to whom all correspondence and reprint requests should be addressed: Mário J. A. Saad, MD, Departamento de Clínica Médica, FCM–UNICAMP, Campinas, SP, 13081-970, Brasil.

Results

Insulin-Stimulated IRS-1 Phosphorylation and Association with SHP2 in Liver and Muscle of STZ-Treated Rats

Figure 1 summarizes the protocol for assessing insulin signaling in the STZ-treated rats. Control and STZ-treated rats were injected with saline or insulin, and after 30 s and 90 s, liver and muscle, respectively, were removed and homogenized as described in the Materials and Methods section. The extracts were immunoprecitated with specific antibodies and then submitted to sodium dodecyl sulfate–polyacrylamide gel electrophoresis (SDS-PAGE) under reducing conditions and were blotted onto nitrocellulose membranes. These blots were subsequently analyzed using antiphosphotyrosine, anti-SHP2, and anti-PI 3-kinase antibodies.

In liver samples previously immunoprecipitated with anti-IRS-1 antibody and immunoblotted with antiphosphotyrosine antibody, there was a clear increase in insulin-stimulated IRS-1 phosphorylation in STZ-treated rats compared to controls (STZ, 141 ± 12% vs control, 100 ± 5%; $p < 0.05$) (Fig. 1A). The level of IRS-1 protein expression did not change in the liver of STZ-treated rats when compared to the controls (Fig. 1B). IRS-1 can bind and activate other proteins, including the phosphotyrosine phosphatase SHP2. We stripped these nitrocellulose membranes and incubated them with anti-SHP2 antibody. The results demonstrated that insulin-induced IRS-1/SHP2 association in liver of diabetic animals was similar to that of control rats (Fig. 1C). Whole tissue extracts submitted to immunoblotting with anti-SHP2 antibody showed that the expression of this protein did not change in the liver of rats treated with STZ, compared to controls (Fig. 1D). There is high-affinity interaction between IRS-1 and the 85-kDa subunit of the PI 3-kinase (PI3K) such that both proteins can be coprecipitated by antibodies to either protein. When blots that had been previously immunoprecipitated with anti-IRS-1 antibody were subsequently incubated with PI 3-kinase antibody, there was an increase in insulin-induced IRS-1/PI 3-kinase association in liver of STZ-diabetic rats when compared to the controls (STZ, 120 ± 6% vs control, 100 ± 4%; $p < 0.05$) (Fig. 1E). In liver of STZ-treated rats, there was no change in the PI 3-kinase protein expression (Fig. 1F). We analyzed the insulin-induced AKT/PKB serine phosphorylation in whole-tissue extract using an antiphospho-AKT antibody. Based on immunoreactivity, the insulin-induced AKT/PKB phosphorylation was decreased in liver of STZ-treated rats compared to the controls (STZ, 45 ± 6% vs control, 100 ± 8%; $p < 0.05$) (Fig. 1G). There was no change in the AKT protein expression in the liver of STZ-treated rats when compared to the controls (Fig. 1H).

In samples from muscle of STZ-treated rats, the results were similar to that observed in the liver. There was an increase in insulin-induced IRS-1 phosphorylation in muscle of STZ-treated rats compared to control animals (STZ, 191 ± 14% vs control, 100 ± 10%; $p < 0.05$) (Fig. 2A). There was no change in IRS-1 protein expression in muscle of diabetic animals (Fig. 2B). Figure 2C shows that there was no change in insulin-induced IRS-1/ SHP2 association in muscle of rats treated with STZ compared to controls. There was also no change in SHP2 protein expression in muscle of diabetic animals (Fig. 2D). There was an increase in insulin-induced IRS-1/PI 3-kinase (PI3K) association in muscle of rats treated with STZ when compared to the controls (STZ, 130 ± 5% vs control, 100 ± 5%; $p < 0.05$) (Fig. 2E). PI 3-kinase protein expression in muscle of STZ-treated rats was not significantly different from that seen in the respective controls, before and after insulin stimulation (Fig. 2F). The insulin-induced AKT/PKB phosphorylation in muscle of STZ-treated rats was reduced compared to the control value (STZ, 30 ± 7% vs control, 100 ± 9%; $p < 0.05$) (Fig. 2G), but AKT protein expression did not change in the muscle of STZ-treated rats compared to controls (Fig. 2H).

Insulin-Stimulated IRS-1 Phosphorylation and Association with SHP2 in Liver and Muscle of Epinephrine-Treated Rats

After epinephrine treatment, changes were observed in insulin-stimulated phosphorylation of IRS-1 in liver. Figure 3A shows that insulin-induced IRS-1 phosphorylation was reduced in epinephrine-treated rats compared to controls (Epi, 37 ± 3% vs control, 100 ± 2%; $p < 0.05$). There was no change in IRS-1 protein expression in the liver of rats treated with epinephrine when compared to controls (Fig. 3B). After insulin stimulation, IRS-1 is coprecipitated with SHP2 and this association was reduced in the liver of epinephrine-treated compared to control animals (Epi, 48 ± 3% vs control, 100 ± 7%; $p < 0.05$) (Fig. 3C). However, using a specific anti-peptide antibody against SHP2, the level of this protein was found to be unchanged in the liver of rats treated with epinephrine (Fig. 3D). The results also demonstrated that insulin-induced IRS-1/PI 3-kinase (PI3K) association was reduced in liver of epinephrine-treated rats compared to controls (Epi, 45 ± 3% vs control, 100 ± 4%; $p < 0.05$) (Fig. 3E), without changes in the PI 3-kinase protein level (Fig. 3F). The AKT/PKB phosphorylation induced by insulin was significantly reduced in the liver of epinephrine-treated rats (Epi, 40 ± 5% vs control, 100 ± 6%; $p < 0.05$) (Fig. 3 G), but AKT protein expression was unchanged (Fig. 3H).

Figure 4A shows that there was a marked reduction in insulin-stimulated IRS-1 tyrosine phosphorylation in the muscle of epinephrine-treated rats compared to controls (Epi, 37 ± 9% vs control, 100 ± 9%; $p < 0.005$). There was no change in the IRS-1 protein expression in muscle of rats treated with epinephrine (Fig. 4B). The association of IRS-1 with SHP2 after insulin stimulation was reduced in the muscle of epinephrine-treated rats (Epi, 40 ± 9% vs control, 100 ± 9%; $p < 0.05$) (Fig. 4C), without changes in SHP2 protein level (Fig. 4D). The IRS-1/PI 3-kinase (PI3K) association was also reduced in the muscle of epinephrine-treated rats

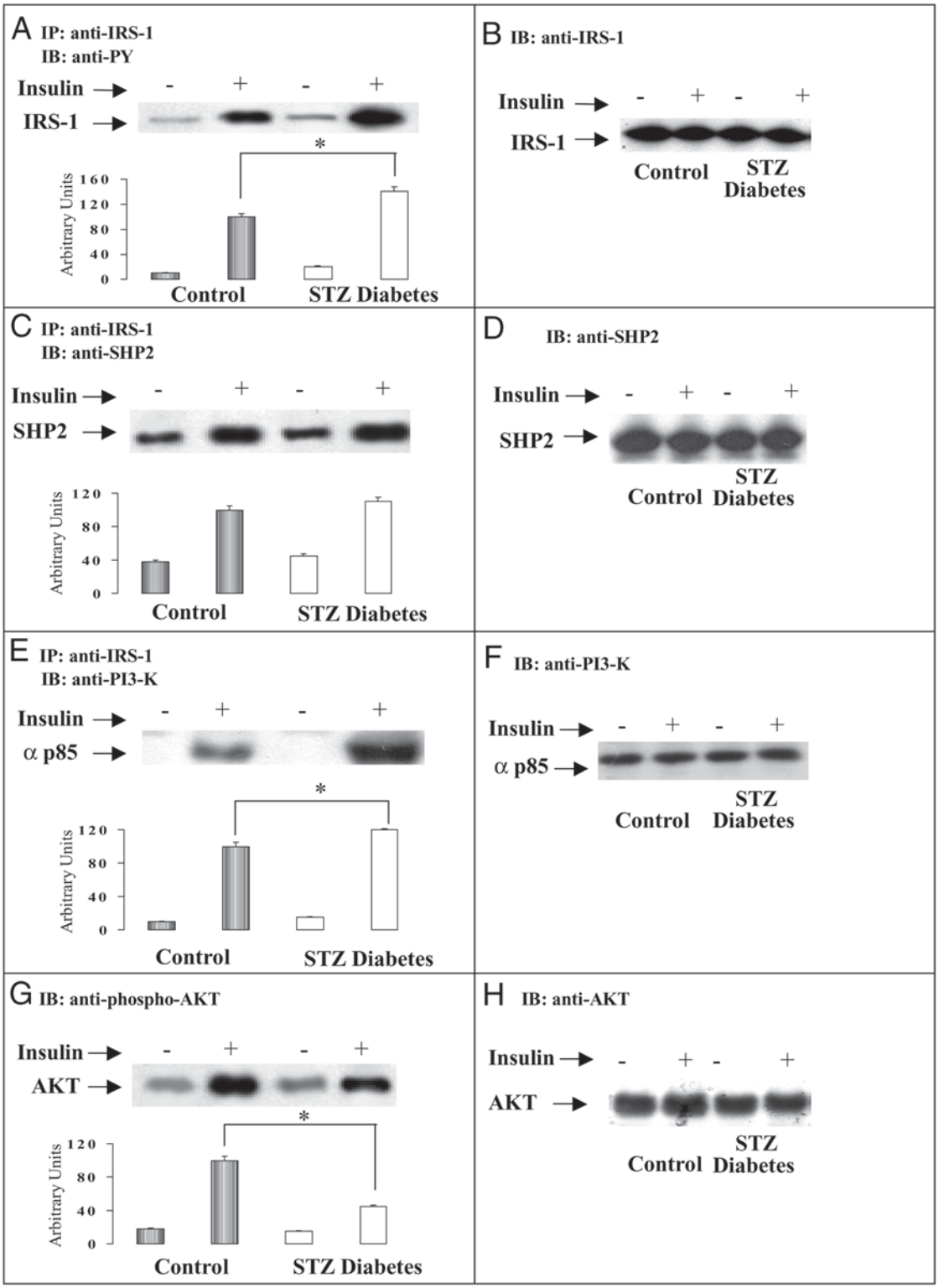

Fig. 1. Insulin-stimulated IRS-1 tyrosine phosphorylation, association of this substrate with SHP2 and PI3K, and AKT phosphorylation in the liver of control and STZ diabetic rats. Liver extracts from rats injected with saline (–) or insulin (+) were prepared as described in the Materials and Methods section. Tissue extracts were immunoprecipitated with anti-IRS-1 (2 μg/mL) and immunoblotted with anti-PY (1 μg/mL) (**A**). The same blot was reprobed with anti-SHP2 (1 μg/mL) (**C**) and anti-PI3K (1 μg/mL) (**E**). Equal quantities of lysate protein were run on SDS-PAGE, and following transfer to nitrocellulose, blots were probed with anti-IRS-1 (1 μg/mL) (**B**), anti-SHP2 (1 μg/mL) (**D**), anti-PI3K (1 μg/mL) (**F**), anti-phospho-AKT (1 μg/mL) (**G**), and anti-AKT (1 μg/mL) (**H**). The values are represented as the mean ± SEM of scanning densitometry of six experiments. The black bars represent the control group and the white bars represent the STZ-treated group. $*p < 0.05$.

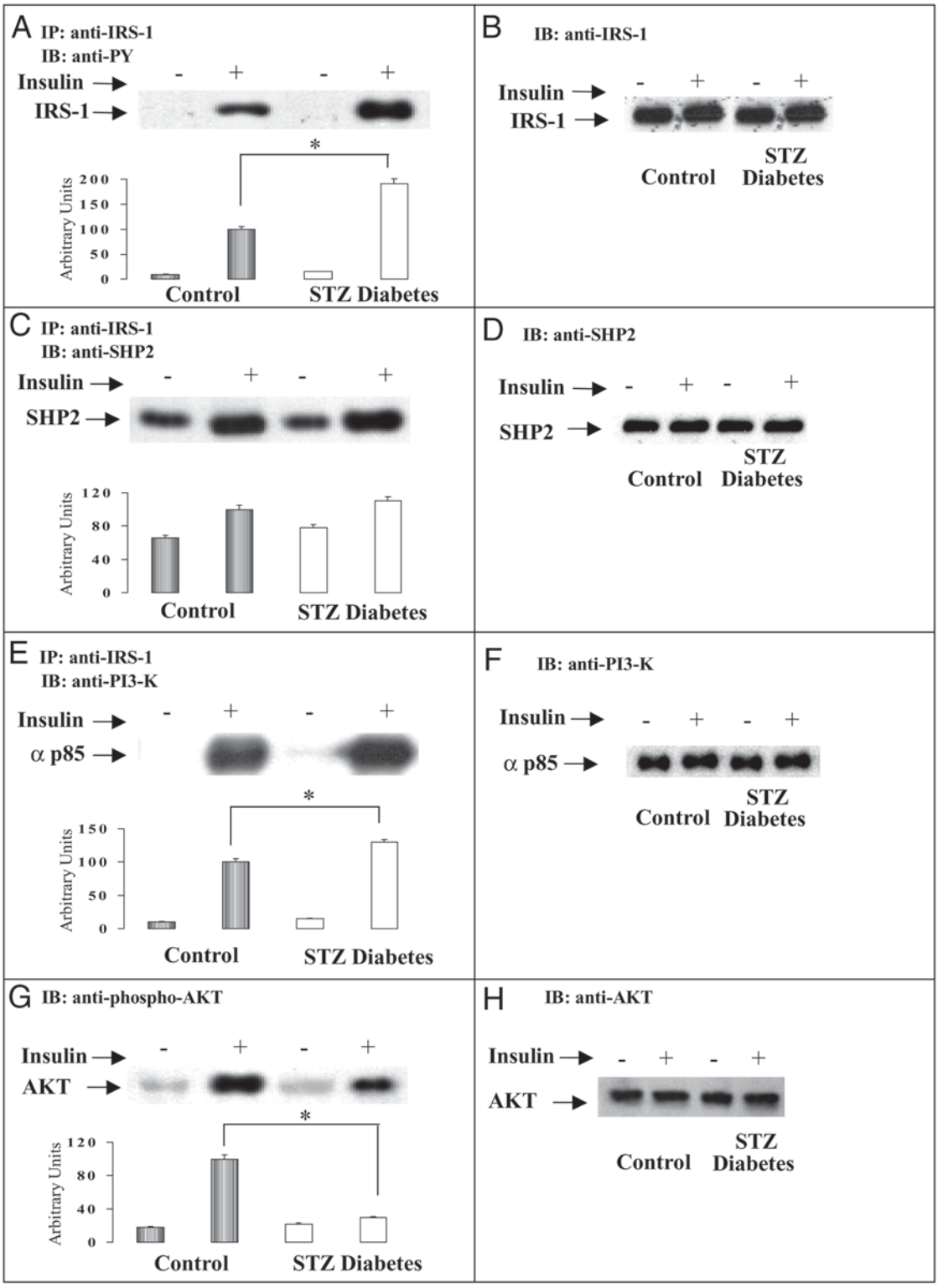

Fig. 2. Insulin-stimulated IRS-1 tyrosine phosphorylation, association of this substrate with SHP2 and PI3K, and AKT phosphorylation in the muscle of control and STZ diabetic rats. Muscle extracts from rats injected with saline (–) or insulin (+) were prepared as described in the Material and Methods section. Tissue extracts were immunoprecipitated with anti-IRS-1 (2 μg/mL) and immunoblotted with anti-PY (1 μg/mL) (**A**). The same blot was reprobed with anti-SHP2 (1 μg/mL) (**C**) and anti-PI3K (1 μg/mL) (**E**). Equal quantities of lysate protein were run on SDS-PAGE, and following transfer to nitrocellulose, blots were probed with anti-IRS-1 (1 μg/mL) (**B**), anti-SHP2 (1 μg/mL) (**D**), anti-PI3K (1 μg/mL) (**F**), anti-phospho-AKT (1 μg/mL) (**G**), and anti-AKT (1 μg/mL) (**H**). The values are represented as the mean ± SEM of scanning densitometry of six experiments. The black bars represent the control group and the white bars represent the STZ-treated group. *$p < 0.05$.

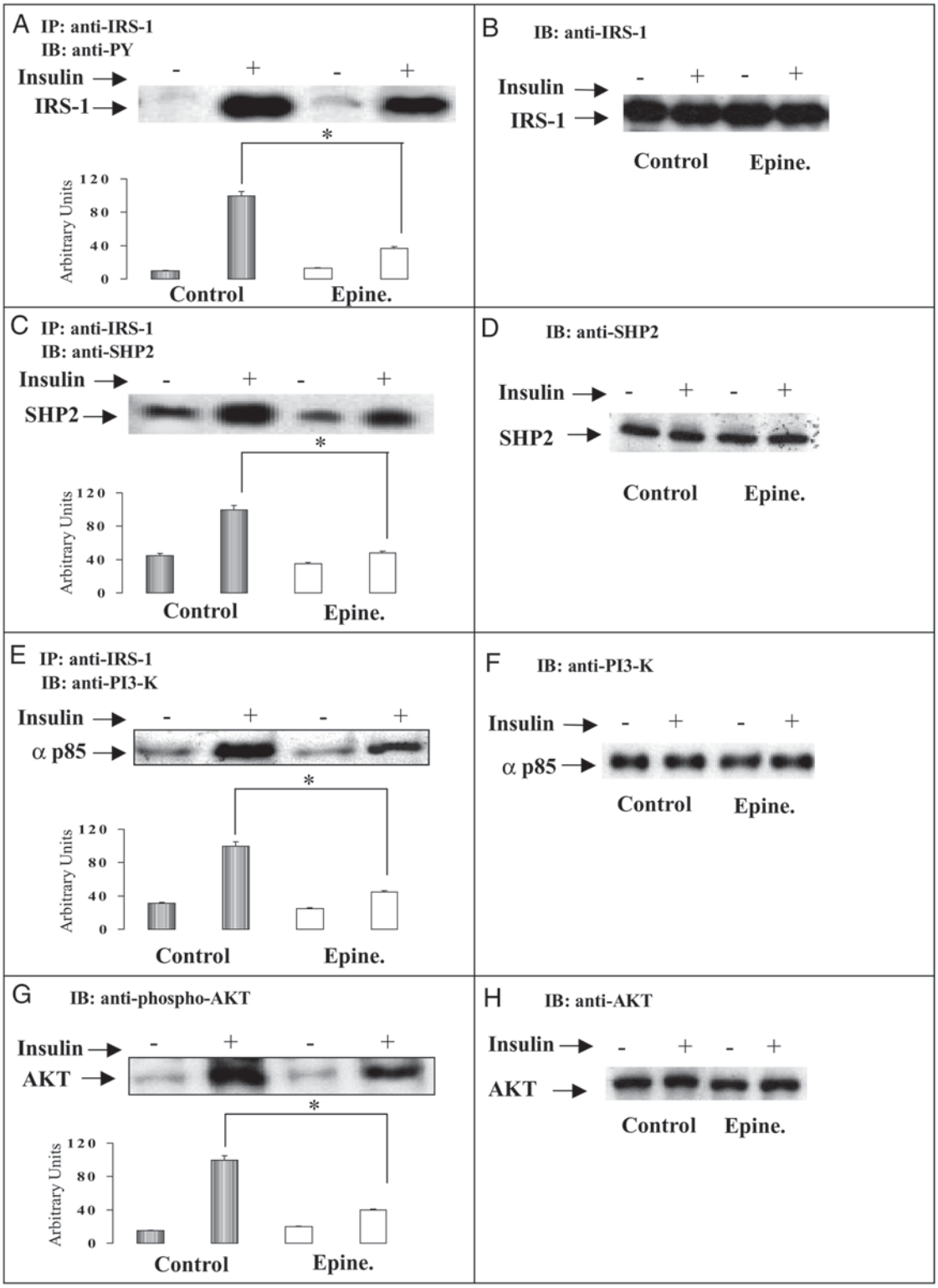

Fig. 3. Insulin-stimulated IRS-1 tyrosine phosphorylation, association of this substrate with SHP2 and PI3K, and AKT phosphorylation in the liver of control and epinephrine-treated rats. Liver extracts from rats injected with saline (–) or insulin (+) were prepared as described in the Material and Methods section. Tissue extracts were immunoprecipitated with anti-IRS-1 (2 µg/mL) and immunoblotted with anti-PY (1 µg/mL) (**A**). The same blot was reprobed with anti-SHP2 (1 µg/mL) (**C**) and anti-PI3K (1 µg/mL) (**E**). Equal quantities of lysate protein were run on SDS-PAGE, and following transfer to nitrocellulose, blots were probed with anti-IRS-1 (1 µg/mL) (**B**), anti-SHP2 (1 µg/mL) (**D**), anti-PI3K (1 µg/mL) (**F**), anti-phospho-AKT (1 µg/mL) (**G**), and anti-AKT (1 µg/mL) (**H**). The values are represented as the mean ± SEM of scanning densitometry of six experiments. The black bars represent the control group and the white bars represent the epinephrine-treated group. $*p < 0.05$.

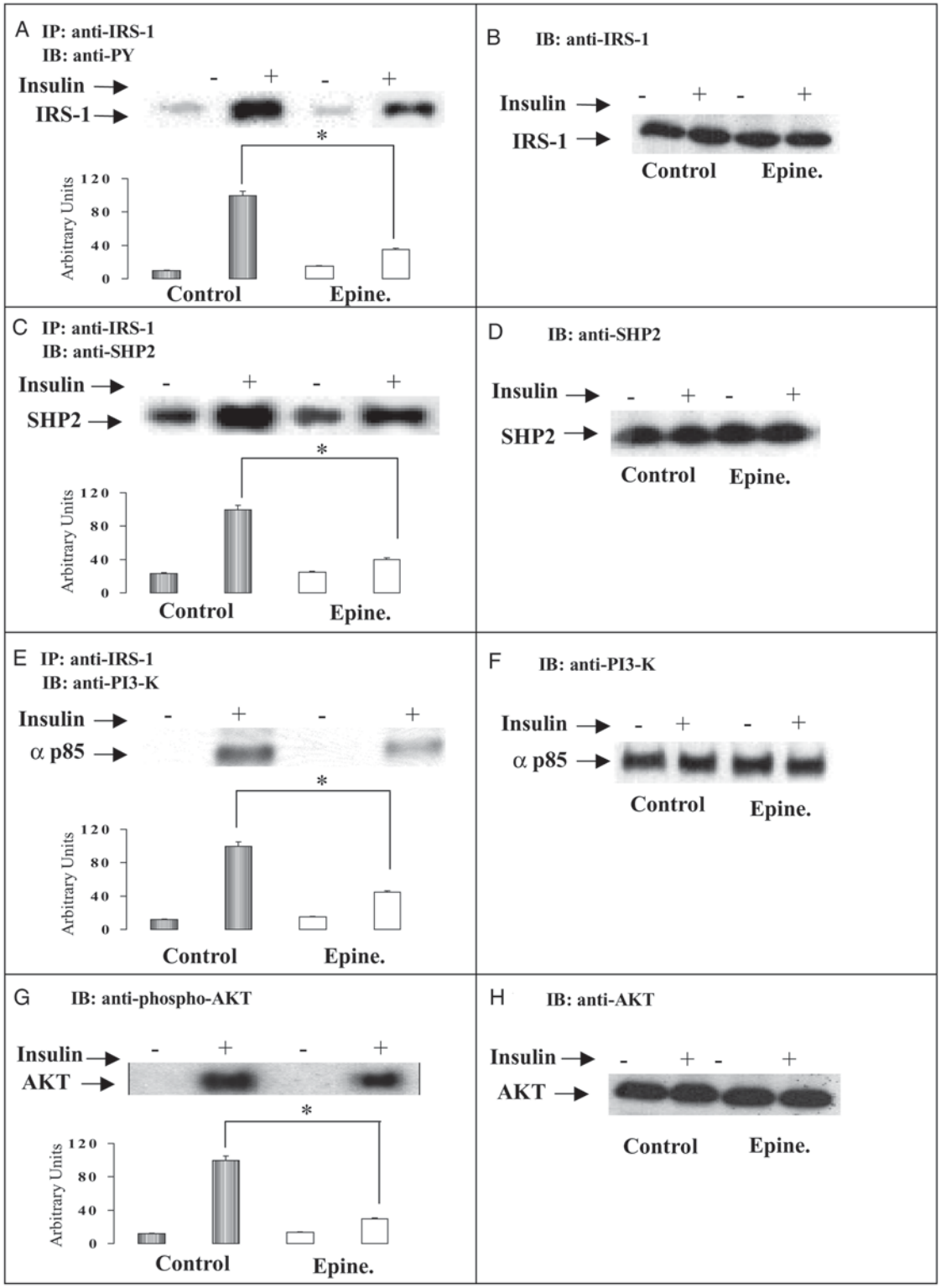

Fig. 4. Insulin-stimulated IRS-1 tyrosine phosphorylation, association of this substrate with SHP2 and PI3K, and AKT phosphorylation in the muscle of control and epinephrine-treated rats. Muscle extracts from rats injected with saline (–) or insulin (+) were prepared as described in the Material and Methods section. Tissue extracts were immunoprecipitated with anti-IRS-1 (2 μg/mL) and immunoblotted with anti-PY (1 μg/mL) (**A**). The same blot was reprobed with anti-SHP2 (1 μg/mL) (**C**) and anti-PI3K (1 μg/mL) (**E**). Equal quantities of lysate protein were run on SDS-PAGE, and following transfer to nitrocellulose, blots were probed with anti-IRS-1 (1 μg/mL) (**B**), anti-SHP2 (1 μg/mL) (**D**), anti-PI3K (1 μg/mL) (**F**), anti-phospho-AKT (1 μg/mL) (**G**), and anti-AKT (1 μg/mL) (**H**). The values are represented as the mean ± SEM of scanning densitometry of six experiments. The black bars represent the control group and the white bars represent the epinephrine-treated group. *$p < 0.05$.

compared to controls (Epi 45 ± 4% vs control, 100 ± 6%; $p < 0.05$) (Fig. 4E). In the muscle of epinephrine rats, there was no change in PI 3-kinase protein expression compared to the controls (Fig. 4F). The phosphorylation of AKT/PKB was reduced in the muscle of rats treated acutely with epinephrine (Epi, 30 ± 6% vs control, 100 ± 4%; $p < 0.05$) (Fig. 4G), without changes in AKT protein expression (Fig. 4H).

Insulin-Stimulated IRS-1 Phosphorylation and Association with SHP2 in the Liver and Muscle of 2-mo-Old or 20-mo-Old Rats

To better define the effect of aging on IRS-1 phosphorylation, we performed a Western blot analysis of the tyrosyl-phosphorylated proteins in anti-IRS-1 immunoprecipitates before and after insulin stimulation in animals 2 and 20 mo of age. After insulin stimulation, there was a decrease in IRS-1 phosphorylation in liver of 20-mo-old rats compared to controls (20M, 36 ± 7% vs 2M, 100 ± 8%; $p < 0.05$) (Fig. 5A). Figure 5B shows that there was no change in IRS-1 protein expression in the liver of 20-mo-old rats compared to controls. Insulin-induced IRS-1/SHP2 association was increased in the liver of 20-mo-old rats compared to 2-mo-old rats (20M, 155 ± 9% vs 2M, 100 ± 7%; $p < 0.05$) (Fig. 5C). Aging also did not significantly change SHP2 protein expression in liver (Fig. 5D). The association of IRS-1 with PI 3-kinase after insulin stimulation was reduced in the liver of 20-mo-old rats compared to 2-mo-old rats (20M, 35 ± 3% vs 2M, 100 ± 5%; $p < 0.05$) (Fig. 5E). The insulin-induced AKT/PKB phosphorylation was unchanged in the liver of aging rats when compared to the controls (Fig. 5G). There was no change in AKT protein levels in the liver of 20-mo-old rats compared to controls (Fig. 5H).

As in the liver, there was a decrease in insulin-stimulated IRS-1 tyrosine phosphorylation in the muscle of 20-mo-old rats when compared to 2-mo-old rats (20M, 50 ± 7% vs 2M, 100 ± 7%; $p < 0.005$) (Fig. 6A). However, in this tissue, IRS-1 protein expression was also reduced in aging rats (20M, 44 ± 3% vs 2M, 100 ± 5%; $p < 0.005$) (Fig. 6B). To examine the association of IRS-1 with SHP2, blots of samples that had been previously immunoprecipitated with anti-IRS-1 antibodies were incubated with anti-SHP2 antibody. There was a decrease in insulin-induced IRS-1/SHP2 association in the muscle of 20-mo-old rats (20M, 52 ± 6% vs 2M, 100 ± 6%; $p < 0.05$) (Fig. 6C), without changes in the SHP2 protein level (Fig. 6D). There was also a decrease in insulin-induced IRS-1/PI 3-kinase association in the muscle of 20-mo-old rats when compared to 2-mo-old rats (20M, 25 ± 4% vs 2M, 100 ± 5%; $p < 0.05$) (Fig. 6E). PI 3-kinase protein expression in muscle of 20-mo-old rats was not significantly different from that seen in the respective controls, before and after insulin stimulation (Fig. 6F). In muscle, insulin-induced AKT/PKB phosphorylation was reduced in the 20-mo-old rats when compared to 2-mo-old rats (20M, 50 ± 6% vs 2M, 100 ± 7%; $p < 0.05$) (Fig. 6G). There was no change in the AKT protein expression in the muscle of these animals (Fig. 6H).

Discussion

The molecular events linking the insulin receptor tyrosine kinase to its final cellular actions is a matter of continuing investigation. In the past 10 yr, several of the early steps in the cascade of insulin action have been characterized at a molecular level. After insulin binding, the activated insulin receptor kinase catalyzes the tyrosine phosphorylation of a protein termed IRS-1. IRS-1 has been shown to be a direct substrate of the insulin receptor both in vivo and in vitro and has several potential serine, threonine, and tyrosine phosphorylation sites *(1,6)*. Following its phosphorylation, IRS-1 can associate with proteins containing SRC homology 2 (SH2) domains through specific tyrosyl phosphorylation sites *(18)*. In cultured cells, phosphorylated IRS-1 associates with lipid-metabolizing enzyme PI 3-kinase, with Nck, Grb2, and the phosphotyrosine phosphatase SHP2 *(18)*.

We have recently demonstrated that SHP2 associates with phosphorylated IRS-1 in the liver and muscle of rats *(14)*. In cultured cells, it has been shown that SHP2 is activated during association with IRS-1. Although the effect of IRS-1/SHP2 association on signal transmission is not completely known, there is a possibility that this interaction autoregulates IRS-1 phosphorylation. The tyrosine phosphatase SHP2 may dephosphorylate signaling intermediates located either in the IRS-1 signaling complex or at distant sites, thus down-regulating signaling *(18,19)*. On the other hand, there is evidence suggesting that SHP2 plays an important role in insulin-induced transcripition of an immediate-early gene such as Glut 1, which is crucial for basal glucose transport in muscles and adipocytes *(20)*. In addition, Maegawa et al. *(21)* recently demonstrated that inhibition of endogenous SHP2 function impaired insulin sensitivity on glucose metabolism in transgenic mice, suggesting that SHP2 may modulate insulin signaling in target tissues. However, the regulation of IRS-1/SHP2 association in animal models of insulin resistance was not yet known. In the present study, we investigated IRS-1/SHP2 association in the liver and muscle of rats in three situations of insulin resistance that course with altered IRS-1 tyrosine phosphorylation. A summary of the results is presented in Table 1.

Streptozotocin diabetes is characterized by insulin deficiency and insulin resistance. The molecular mechanisms responsible for this insulin resistance is not clear, but at least defects in early steps in insulin action have been demonstrated. We have previously described that in the liver and muscle of STZ-diabetic animals with the same severity and duration of diabetes as in this study, there is an increase in insulin-induced IRS-1 tyrosine phosphorylation levels and an increase in IRS-1/PI 3-kinase association *(16,22)*. The results of the present study confirmed previous studies and add new information showing that insulin-induced IRS-1/

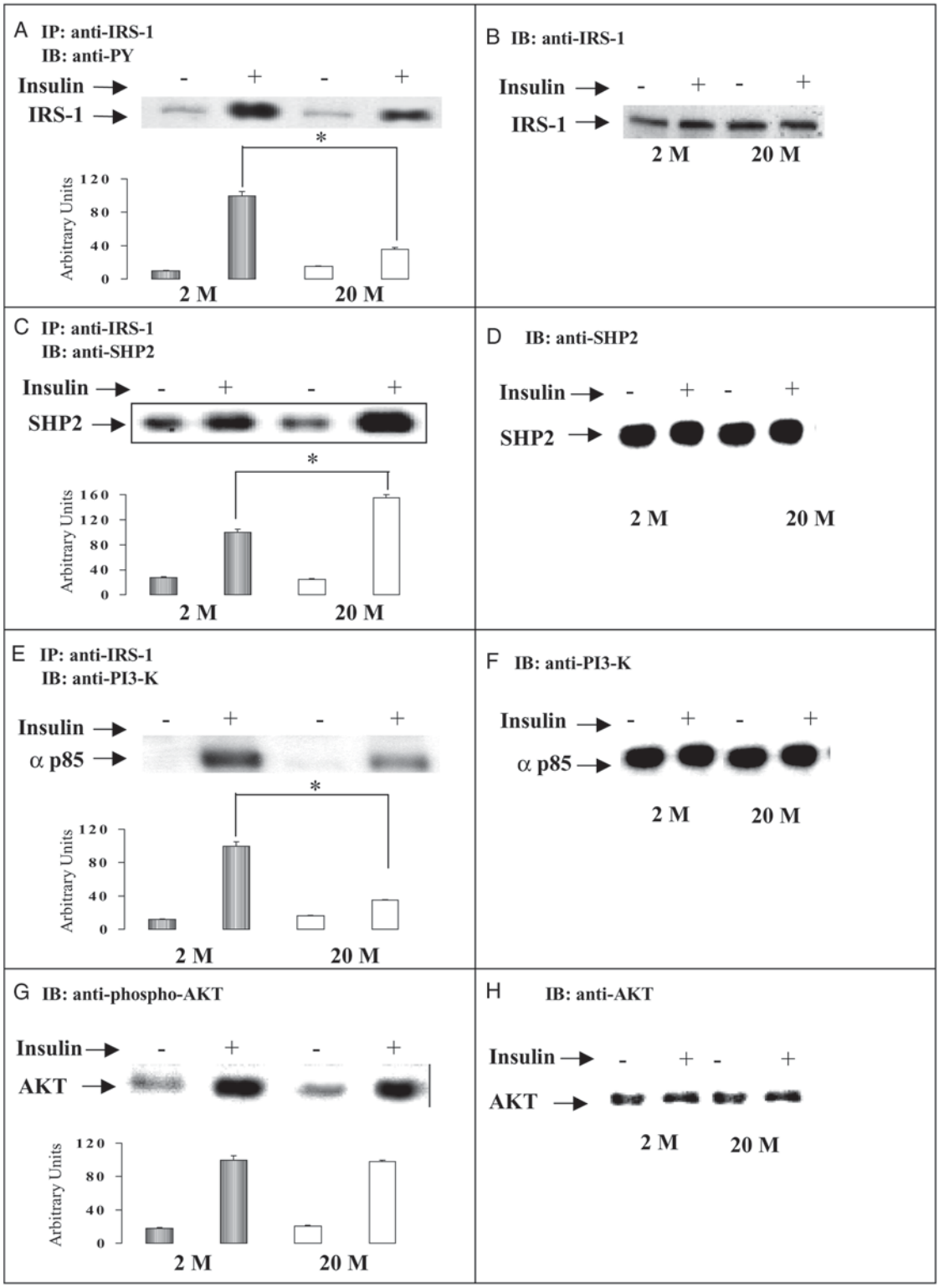

Fig. 5. Insulin-stimulated IRS-1 tyrosine phosphorylation, association of this substrate with SHP2 and PI3K, and AKT phosphorylation in the liver of 2-mo-old or 20-mo-old rats. Liver extracts from rats injected with saline (–) or insulin (+) were prepared as described in the Material and Methods section. Tissue extracts were immunoprecipitated with anti-IRS-1 (2 μg/mL) and immunoblotted with anti-PY (1 μg/mL) (**A**). The same blot was reprobed with anti-SHP2 (1 μg/mL) (**C**) and anti-PI3K (1 μg/mL) (**E**). Equal quantities of lysate protein were run on SDS-PAGE, and following transfer to nitrocellulose, blots were probed with anti-IRS-1 (1 μg/mL) (**B**), anti-SHP2 (1 μg/mL) (**D**), anti-PI3K (1 μg/mL) (**F**), anti-phospho-AKT (1 μg/mL) (**G**), and anti-AKT (1 μg/mL) (**H**). The values are represented as the mean ± SEM of scanning densitometry of six experiments. The black bars represent the 2-mo-old rats group and the white bars represent 20-mo-old rats group. *$p < 0.05$.

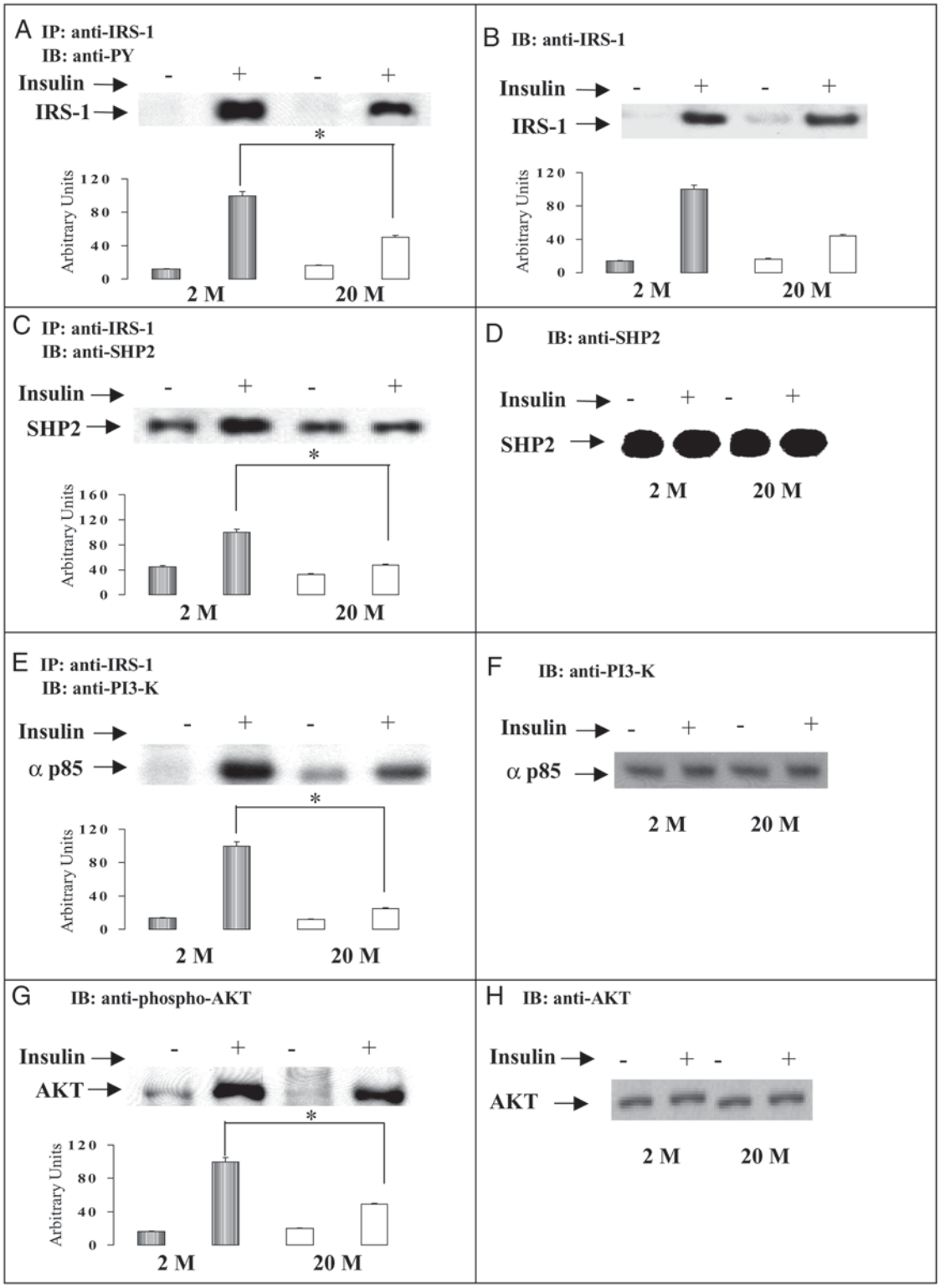

Fig. 6. Insulin-stimulated IRS-1 tyrosine phosphorylation, association of this substrate with SHP2 and PI3K, and AKT phosphorylation in the muscle of 2-mo-old or 20-mo-old rats. Muscle extracts from rats injected with saline (–) or insulin (+) were prepared as described in the Material and Methods section. Tissue extracts were immunoprecipitated with anti-IRS-1 (2 μg/mL) and immunoblotted with anti-PY (1 μg/mL) (**A**). The same blot was reprobed with anti-SHP2 (1 μg/mL) (**C**) and anti-PI3K (1 μg/mL) (**E**). Equal quantities of lysate protein were run on SDS-PAGE and following transfer to nitrocellulose, blots were probed with anti-IRS-1 (1 μg/mL) (**B**), anti-SHP2 (1 μg/mL) (**D**), anti-PI3K (1 μg/mL) (**F**), anti-phospho-AKT (1 μg/mL) (**G**), and anti-AKT (1 μg/mL) (**H**). The values are represented as the mean ± SEM of scanning densitometry of six experiments. The black bars represent the 2-mo-old rats group and the white bars represent 20-mo-old rats group. $*p < 0.05$.

Table 1
Regulation of Proteins Involved in Early Steps of Insulin Action in Liver and Muscle of Three Animal Models of Insulin Resistance: STZ Diabetic Rats, Epinephrine-Treated Rats, and Aging

	STZ		Epinephrine		Aging	
	Liver	Muscle	Liver	Muscle	Liver	Muscle
IRS-1 protein	↔	↔	↔	↔	↔	↓↓
AKT protein	↔	↔	↔	↔	↔	↔
SHP2 protein	↔	↔	↔	↔	↔	↔
PI 3-kinase protein	↔	↔	↔	↔	↔	↔
IRS-1/phosphorylation	↑↑	↑↑	↓↓	↓↓	↓↓	↓↓
IRS-1/PI 3-kinase association	↑↑	↑↑	↓↓	↓↓	↓↓	↓↓
IRS-1/SHP2 association	↔	↔	↓↓	↓↓	↑↑	↓↓
AKT phosphorylation	↓↓	↓↓	↓↓	↓↓	↔	↓↓

Note: ↑↑, increase of protein; ↓↓, decrease of protein; ↔, no alteration.

SHP2 association in the liver and muscle of STZ diabetic rats was similar to controls. The IRS-1/PI 3-kinase and IRS-1/SHP2 associations were not influenced by IRS-1, PI 3-kinase, or SHP2 protein levels, which were unchanged in the liver and muscle of these diabetic animals. The mechanism responsible for the differential regulation of IRS-1 associations with these two enzymes is not known, but because there are specific tyrosines in IRS-1 that bind PI 3-kinase or SHP2, we can suggest that in the liver and muscle of STZ diabetic rats the increase in IRS-1 phosphorylation is probably not in tyrosines, which bind SHP2. The increase in IRS-1/ PI 3-kinase association without an increase in IRS-1/SHP2 association may attenuate downstream signaling. It is interesting that AKT phosphorylation was reduced in the liver and muscle of STZ diabetic animals in spite of an increase in IRS-1/PI 3-kinase association.

It has long been known that an excess of epinephrine causes insulin resistance *(23–25)*. High intracellular cyclic AMP levels seem to induce insulin resistance at both receptor and postreceptor levels *(26–28)*. Using purified receptors and artificial substrates in vitro, decreased insulin receptor phosphorylation and kinase activity has been observed as a consequence of increased cAMP and cAMP kinase *(29)*. We have recently demonstrated that in the liver and muscle of rats treated with epinephrine, there is a decrease in insulin-induced insulin receptor and IRS-1 tyrosine phosphorylation and in IRS-1/PI 3-kinase association *(15)*. In the present study, we confirmed the previous data and demonstrated that there is a parallel decrease in IRS-1/SHP2 association in the liver and muscle of rats treated with epinephrine, without changes in IRS-1, PI 3-kinase, SHP2, and AKT protein expression.

The mechanism by which epinephrine reduces IRS-1 tyrosine phosphorylation levels and associations are not known, but at least two possibilities should be considered. First, it is well known that agents that raise intracellular cAMP levels increase phosphorylation of the insulin receptor at serine and threonine residues, reduce insulin-mediated receptor phosphorylation on tyrosine, and inhibit the insulin-dependent tyrosine protein kinase activity of the receptor. Thus, cAMP may attenuate insulin action by altering the state of phosphorylation of the insulin receptor. It is not known whether an increase in intracellular cAMP also induces a serine phosphorylation in IRS-1. However, because insulin receptor kinase activity is reduced, a reduction in IRS-1 phosphorylation and, hence, in the association between IRS-1/PI 3-kinase and IRS-1/ SHP2 are also expected. Another possibility arises from data showing that an increase in cellular cAMP through activation of protein kinase A (PKA) increases the activity of endogenous phosphotyrosine phosphatase (PTPase), thus leading to a sequence of dephosphorylation *(30)*.

It is interesting that insulin-induced AKT phosphorylation was attenuated in epinephrine-treated rats. Recently, AKT activity has been reported to be essential for activation of glycogen synthase by insulin *(12)*. Because AKT phosphorylation correlates with AKT activity, we can suggest that a decrease in insulin-induced AKT phosphorylation may contribute to the insulin resistance observed in epinephrine-treated rats.

The insulin resistance that develops during aging is associated with glucose intolerance. The rate of glycogen synthesis in response to insulin stimulation is markedly decreased in the soleus muscle of 85-wk-old Wistar rats *(31)* and impaired insulin-stimulated glucose uptake as a result of a depletion of the pool of glucose transporters has been observed *(32)*. At high insulin levels, there is no alteration in insulin-induced inhibition of hepatic glucose output, suggesting that the insulin resistance observed in aging is mainly located in skeletal muscle *(17,33,34)*. Carvalho et al. *(17)* demonstrated that in the liver and muscle of old rats, there is a decrease in IRS-1 tyrosine phosphorylation level and a decrease in IRS-1/PI 3-kinase association. Evidence from other sources and using different approaches demonstrated a correlation between PI 3-kinase activity and glucose transport *(34–36)*. Thus, it is reasonable to speculate that the reduction in IRS-1/PI 3-kinase association in old rats may have

a role in the resistance observed in aging. It is interesting that in contrast to IRS-1/PI 3-kinase, which was reduced in both the liver and muscle, insulin-induced IRS-1/SHP2 association showed a tissue-specific regulation, decreasing in muscle and increasing in liver. The mechanisms responsible for these alterations are not established, but the levels of IRS-1 may have a role, because they decrease in the muscle but not in the liver of aging rats as previously demonstrated *(17)* and confirmed in our study.

The existence of alternative substrates and pathways for insulin signaling suggests that compensatory changes in either IRS-1 protein levels or IRS-1/SHP2 associations could minimize the impact of alterations in IRS-1-linked signaling. In aging rats, there is a decrease in AKT phosphorylation in the muscle but not in the liver, which parallel the changes observed in IRS-1/SHP2 association. It is important to emphasize that AKT protein expression was unchanged in the liver and muscle of aging rats.

Because AKT/PKB phosphorylation is related to AKT/PKB activity, we can suggest that in the liver of aging rats, AKT/PKB activity induced by insulin is probably normal, which can contribute to the explanation of the normal suppression of hepatic glucose output during the infusion of high doses of insulin *(33,37)*. On the other hand, the reduction in AKT phosphorylation in the muscle of aging rats may have a role in the reduced insulin sensitivity observed in these animals.

Taking these three models of insulin resistance together, we can suggest that insulin-induced IRS-1/PI 3-kinase association has a close correlation with IRS-1 tyrosine phosphorylation levels, but insulin-induced IRS-1/SHP2 association did not parallel IRS-1 phosphorylation, with different behavior in the animal models and with a tissue-specific regulation in aging. The integration of the behavior of IRS-1/PI 3-kinase association with IRS-1/SHP2 association may be important for insulin signaling downstream as AKT phosphorylation.

Materials and Methods

Materials

The reagents and apparatus for SDS-PAGE and immunoblotting were from Bio-Rad (Hercules, CA). Tris, [hydroxymethyl] amino-methane (Tris) phenylmethylsulfonylfluoride (PSMF), silicone, dithiothreitol (DTT), Triton X-100, Tween-20, and glycerol were from Sigma Chemical Co. (St. Louis, MO, USA) and aprotinin was from Bayer (São Paulo, Brazil). Sodium amobarbital was from Lilly. Human recombinant insulin (Humulin R) was from Biobrás (Montes Claros, Brazil). [^{125}I]Protein A was from Amersham (Amersham, Aylesbury, UK) and protein A–Sepharose 6 MB was from Pharmacia (Uppsala, Sweden). Nitrocellulose membrane was from Amersham (Amersham, Buckinghamshire, UK). Male Wistar rats were from the UNICAMP Central Breeding Center. Monoclonal antiphosphotyrosine antibody (αPY/clone 4G10) was from Upstate Biotechnology Inc. (UBI, Lake Placid, NY). Anti-IRS-1 (αIRS-1/C20) and anti-SHP2 (αSHP2/C-18) and anti-AKT protein antibodies were from Santa Cruz Biotechnology (Santa Cruz, CA). Anti-phospho-AKT antibody was from New England Biolabs (Hitchin, UK) and anti-PI 3-kinase (α p85) antibody was from Upstate Biotechnology Inc.

Animals

Male Wistar rats, 6-wk-old, were divided into two groups and the studies were performed in parallel using the control and treated rats. All groups received standard rodent chow and water *ad libitum*. Diabetes mellitus was induced with a single dose of streptozotocin (Sigma; 60 mg/kg body weight in citric buffer, pH 4.5) and age-matched rats received an equivalent volume of citric buffer, pH 4.5. Rats were used for experiments 7 d after receiving STZ injection. In another series of experiments, anesthetized rats were injected with epinephrine (25 μg/kg/ip) or an equal volume of saline (control group) and the animals were used 5 min later. In order to investigate the effect of aging on insulin signal transduction, we used male Wistar rats divided into two groups by age 2 mo old (control) or 20 mo old. The groups were fed standard rodent chow and water *ad libitum*. In all groups, the rats were fasted for 12–14 h before being used, as described in the following subsection. All experiments with animals were approved by the Committee of the State University of Campinas (UNICAMP).

Methods

Rats were anesthetized with sodium amobarbital (15 mg/kg/ip) and were used 10–15 min later, as soon as anesthesia was ensured by the loss of pedal and corneal reflexes. The abdominal cavity was opened, the portal vein exposed, and 0.5 mL of normal saline (0.9% NaCl) with or without 6 μg of insulin was injected. After 30 s, the liver was removed, and at 90 s, the hindlimb muscle was removed, minced coarsely and homogenized immediately in extraction buffer (1% Triton X-100, 100 m*M* Tris, pH 7.4, containing 100 m*M* sodium pyrophosphate, 100 m*M* sodium fluoride, 10 m*M* EDTA, 10 m*M* sodium vanadate, 2 m*M* PSMF, and 0.1 mg of aprotinin/mL) at 4ºC with a Polytron PTA 20S homogenizer (Brinkmann Instruments model PT 10/35) operated at maximum speed for 30 s. Both extracts were centrifuged at 30,000*g* and 4ºC in a Beckman 70.1 Ti rotor (Palo Alto, CA) for 45 min to remove insoluble material, and the supernatant of these tissues was used for imunoprecipitation with anti-IRS-1 antibody and protein A–Sepharose-6 MB.

The samples were treated with Laemmli sample buffer *(39)* containing 100 m*M* DTT and heated in a boiling-water bath for 4 min. SDS-PAGE (6.5% Tris/acrylamide) was carried. For total extracts, similar-sized aliquots (250 μg protein) were subjected to SDS-PAGE. Electrotransfer of proteins from the gel to nitrocellulose membrane was performed for 2 h at 120 V (constant) in a Bio-Rad miniature transfer appa-

ratus (Mini-protean), as previously described by Towbin et al. *(40)*, except for the addition of 0.02% SDS and β-mercaptoethanol to the transfer buffer to enhance the elution of high-molecular-mass protein. Nonspecific protein binding to the nitrocellulose membranes was reduced by preincubating the membrane for 2 h at 22ºC in blocking buffer (3% bovine serum albumin [BSA], 10 m*M* Tris, 150 m*M* NaCl, and 0.02% Tween-20). The prestained molecular-mass standards used were myosin (205 kDa), β-galactosidase (116 kDa), BSA (80 kDa), and ovalbumin (49.5 kDa). The membranes were then incubated with anti-phosphotyrosin, anti-SHP2 or anti-phospho-AKTantibodies, diluted in blocking buffer (0.3% BSA instead of nonfat dry milk) for 4 h at 22ºC, washed again three times (10 min each) in blocking buffer without milk, and then incubated with 2 µCi of [^{125}I]protein A (30 µCi/µg) in 10 mL of blocking buffer (1% nonfat dry milk) for 2 h at 22ºC followed by a final wash. [^{125}I]Protein A bound to the antibodies was detected by autoradiography using preflashed Kodak XAR film with Cronex Lightning Plus intensifying screens at –70ºC for 12–120 h. Images of the developed autoradiographs were scanned (Hewlett Packard ScanJet 5p) into Corel Photo Paint 5.0 on a Compaq Presario computer and band intensities were quantified by optical densitometry (NIH Image Analysis System). Preliminary assays were performed to ensure autoradiographic readings in the linear range.

Statistical Analysis

The experiments were performed by studying all groups of animals in parallel (n = 6 animals/group). Comparisons were done using Student's unpaired t-test (Statview software, Abacus). Densitometric values are expressed as a percentage of the mean value for the insulin-stimulated control (100%) of each experimental group. The level of significance used was $p < 0.05$.

Acknowledgments

We thank Mr. L. Janeri and Mrs. R. Pithon for technical assistance. This work was supported by Fundação de Amparo à Pesquisa do Estado de São Paulo (FAPESP).

References

1. White, M. F. and Kahn, C. R. (1994). *J. Biol. Chem.* **269,** 1–5.
2. Sun, X. J., Rothenberg, P. L., Kahn, C. R., Backer, J. M., Araki, E., Wilden, P., et al. (1991). *Nature* **352,** 73–77.
3. White, M. F., Maron, R., and Kahn, C. R. (1985). *Nature* **318,** 183–186.
4. Backer, J. M., Myers, M. G. Jr., Shoelson, S. E., Chin, D. J., Sun, X. J., Miralpeix, M., et al. (1992). *EMBO J.* **11,** 3469–3479.
5. Harari, Y. R., Tzahar, E., Nadiv, O., Rothenberg, Roberts, C. T. Jr., LeRoith, D., et al. (1992). *J. Biol. Chem.* **267,** 17,483–17,486.
6. Myers, M. G. Jr. and White, F. M. (1996). *Annu. Rev. Pharmacol. Toxicol.* **36,** 615–658.
7. Cheatham, B. and Khan, C. R. (1995). *Endocrinol. Rev.* **16,** 117–142.
8. Cohen, P., Alessi, D. R., and Cross, D. A. E. (1997). *FEBS Lett.* **410,** 3–10.
9. Klippel, A., Kavanaugh, W. M., Pot, D., and Williams, L. T. (1997). *Mol. Cell. Biol.* **17,** 338–344.
10. Tanti, J. L., Grillo, S., Gremeaux, T., Coffer, P. J., Van Obberghen, E., and Le-Marchand-Brustel, Y. (1997). *Endocrinology* **138,** 2005–2010.
11. Downward, J. (1998). *Science* **279,** 673–674.
12. Kitamura, T., Ogawa, W., Sakaue, H., Hino, Y., Kuroda, K., Takata, M., et al. (1998). *Mol. Cell. Biol.* **18,** 3708–3717.
13. Kuhné, M. R., Pawson, T., Lienhard, G. E., and Feng, G. S. (1993). *J. Biol. Chem.* **268,** 11,479–11,481.
14. Lima, M. H. M., Zambelli, J. E., Carvalho, C. R., and Saad, M. J. A. (1998). *Braz. J. Med. Biol. Res.* **31,** 1409–1413.
15. Saad, M. J. A., Hartmann, L. G. C., Carvalho, D. S., Galoro, A. O., Brenelli, S. L., and Carvalho, C. R. O. (1995). *Endocrine* **3,** 755–759.
16. Folli, F., Saad, M. J. A., Backer, M., and Kahn, R. (1993). *J. Clin. Invest.* **92,** 1787– 1794.34.
17. Carvalho, C. R. O., Brenelli, S. L., Silva, A. C., Nunes, A. L. B, Velloso, L. A., and Saad, M. J. A. (1996). *Endocrinology* **137,** 151–159.
18. Yamauchi, K., Ribon, V., Saltiel, A. R., and Pessin, J. E. (1995). *J. Biol. Chem.* **270,** 17,716–17,722.
19. Milarski, K. L. and Saltiel, A. R. (1994). *J. Biol. Chem.* **269,** 21,239–21,243.
20. Hausdorff, F. S., Bennett, A. M., Neel, B. G., and Birnbaum, M. J. (1995). *J. Biol. Chem.* **270,** 12965–121968.
21. Maegawa, H., Hasegawa, M., Sugai, S., Obata, T., Ugi, S., Morino, K., et al. (1999). *J. Biol. Chem.* **274,** 30236–30243.
22. Saad, M. J. A., Araki, E., Miralpeix, M., Rothenberg, P. L., White, M. F., and Kahn, C. R. (1992). *J. Clin. Invest.* **90,** 1839–1849.
23. Chiasson, J. L., Shikama, H., Chu, D., and Exton, J. H. (1981). *J. Clin. Invest.* **68,** 706–713.
24. Kirsch, D., Kemmeler, W., and Haring, H. U. (1993). *Biochem. Biophys. Res. Commun.* **115,** 389–405.
25. Pessin, J. E., Gitomer, W., Oka, Y., Oppenheimer, C. L., and Czech, M. P. (1983). *J. Biol. Chem.* **258,** 7386–7394.
26. Joost, H. G., Webwe, T. M., Cushman, S. W., and Simpson, I. A. (1986). *J. Biol. Chem.* **261,** 10,033–10,036.
27. Kuroda, M., Honnor, R. C., Cushman, S. W., Londos, C., and Simpson, I. A. (1987). *J. Biol. Chem.* **262,** 245–253.
28. Staudmauer, L. and Rosen, O. M. (1986). *J. Biol. Chem.* **261,** 3402–3407.
29. Wilson, G. F. and Kaczmarek, L. K. (1993). *Nature* **366,** 433–438.
30. Goodman, N. M., Dluz, S. M., McElaney, M. A., Belur, E., and Ruderman, N. B. (1983). *J. Physiol.* **244,** E93–E100.
31. Bader, S., Scholz, R., Kellerer, M., et al. (1992). *Diabetologia* **35,** 712–718.
32. Davidson, M. B. and Karjala, R. G. (1978). *Metabolism* **27,** 1994–2005.
33. Yoshimasa, Y., Yamada, K., Ida, T., Kakehi, T., and Imura, H. (1988). *Am. J. Physiol.* **254,** E92–E98.
34. Cheatham, B., Vlahos, C. J., Cheatham, L., Wang, L., Blenis, J., and Kahn, C. R. (1994). *Mol. Cell. Biol.* **14,** 4902–4911.
35. Quon, M. J., Butte, A. J., Zarnowski, M. J., Sesti, G., Cushman, S. W., and Taylor, S. I. (1995). *J. Biol. Chem.* **269,** 27,920–27,924.
36. Kanai, F., Ito, K., Todaka, M., Hayashi, H., Kamohara, S., Ishii, K., et al. (1993). *Biochem. Biophys. Res. Commun.* **195,** 762–768.
37. Fink, R. I., Kolterman, O. G., Griffin, J., and Olefsky, J. M. (1983). *J. Biol. Chem.* **267,** 17,483–17,486.
38. Laemmli, U. K. (1970). *Nature* **227,** 680–685.
39. Towbin, H., Staehlin, J., and Gordon, J. (1979). *Proc. Natl. Acad. Sci. USA* **76,** 4350–4354.